IJE TRANSACTIONS A: Basics Vol. 34, No. 10, (October 2021) 2280-2293

International Journal of Engineering
Journal Homepage: www.ije.ir

# Comparative Study on Structural Behavior of Reinforced Concrete Straight Beam and Beams with out Plane Parts

M. S. Mohsin, N. A. Alwash, M. M. Kadhum*

*Civil Engineering Department, College of Engineering, Babylon University, Iraq*

*P A P E R I N F O*

*Paper history:*
Received 21 May 2021
Received in revised form 25 June 2021
Accepted 02 July 2021

*Keywords*:
*Concrete Beams*
*Out of Plane Part*
*Normal Strength Concrete*
*Angle of Twist*

*A B S T R A C T*

This paper aims to experimentally investigate and compare the structural behavior of reinforced concrete straight beam and other beams there made with one, two, and three out of plane parts. The study focused on the effect of the number and location of the out plane parts on the beams mid span deflection, and rotation, as well as the ductility index, cracking loads, and failure modes. Four beams were fabricated with a cross-sectional width of 150 mm and a depth of 200 mm, and 2000 mm in length. All the beams were made with normal strength concrete and constant longitudinal reinforcement ratio 0.011 for negative and positive moments. All the beam specimens were clamped by a special steel fixed ends and subjected to the two-point load up to their failure. The obtained results presented that the load bearing capacity of straight beam was higher than the beams with out of plane parts. Furthermore, the beam with two out of plane parts has capacity higher than the beams with one and three out of plane part by 5.86 and 55.07%, respectively. In addition, the results showed that the ductility increased with increasing number of out of plane parts by 5.52%, and 32.71% as copared with the beam with one out of plane part.

***doi***: *10.5829/ije.2021.34.10a.09*

## 1. INTRODUCTION

A reinforced concrete structures can be cast to take the shape required, making it widely used to mix the architectural and structural requirements. It is also maintain the aesthetic of the buildings, because it is yields as rigid members with minimum apparent deflection. In some special cases in low-rise and high-rise buildings inside and outside them, the designer need to change the straight path of the beams to a non-straight path, whether for architectural purposes or to reduce the number of columns to provide a wider utilization of space, like corner beams, balcony beams, grid beams system, zigzag concrete beams, and other architectural application requirements. Examples of this type of members as in Sky House Tokyo in Japan, Complex structural layout in China, Cross-bracing concrete beam in Budapest metro stations, Concrete Balconies in National Theatre, London and Modern concrete buildings with cantilever corner balcony beams as shown in Figure 1. This variation within the axis of the beam led to a change in its structural behavior in terms of its strength including bending, shear, torsion and lateral torsional buckling as compared with the straight members. Therefore, there are researchers studied the structural behavior of the reinforced concrete beams under combined loading of torsion, bending, and shear to evaluate the effect of load application method on the beam .

Owainati [1] studied the effects of using different combinations loadings of torsion, bending and shear with the different torsion to shear ratio, and different ratios of transverse and longitudinal reinforcement on the structural behavior of rectangular reinforced concrete beams that made with a wing loading arms at the front and back sides of the beam to apply the torsional loads. The study concluded that the cracks' shapes and failure mode was affected by the loading type. Moreover, an increase in the ratio of longitudinal and transverse reinforcement enhanced each of the

*Corresponding Author Institutional Email: eng.mohammed.mansour@uobabylon.edu.iq (M. M. Kadhum)

Please cite this article as: M. S. Mohsin, N. A. Alwash, M. M. Kadhum, Comparative Study on Structural Behavior of Reinforced Concrete Straight Beam and Beams with out Plane Parts, International Journal of Engineering, Transactions A: Basics, Vol. 34, No. 10, (2021) 2280-2293

(a) Sky House Tokyo, Japan

(b) Complex structural layout, China

(c) Cross-bracing in Budapest metro stations

(d) Balconies in National Theatre, London

(e) Modern concrete buildings with cantilever corner balcony beams

**Figure 1.** Beam with out of plane parts applications

cracking and ultimate load, but the transverse reinforcement is more effective in increasing the cracking torsional moment. Ali and Anis [2] analyzed the reinforced concrete floor to spandrel beam assembly by experimental work and analytical solution to study the effects of loading arrangement on the structural behavior like flexural strength, torsional capacity and deformations. The structural model loaded by two types of loading, first one by applied concentrated load at mid-span of the floor beam and made the spandrel beam exposed to pure torsional moment, while the second one by applied concentrated load at the joint of floor beam to spandrel beam in addition to first loading and made it exposed to combined loading. According to the load-deflection relationship, the study results showed that the ductility decreased and the angle of twist at the ultimate load increased when the model exposed to the combined loading type two. Kamiński and Pawlak [3] adopted the experimental work and numerical analyses to investigate the load capacity and stiffness of angular and rectangular beams under two types of loading. The first type of loading was a pure torsional moment and the second type was a combined load of a torsional moment plus a shearing force and a bending moment. The analyses results conclude that the load capacity and stiffness of the beams decreased when their exposed to combined loading of both a torsional moment and bending moment as compared with the beams that just loaded with a torsional moment.

ACI 445.1R-12 [4] based on the theoretical and experimental results of many previous researches for the reinforced rectangular concrete beams under three types of loading pure torsion, bending plus torsion, and shear plus torsion and explained that the presence of a bending moment reduced the torsional ductility of the beams and the torsion to bending moment ratio affected on the diagonal compression angle and the pattern of the cracks, the cracks were diagonal on the bottom face under pure torsion, but the cracks angle became normal to the longitudinal axis of the beam under pure bending. Elsayed et al. [5] investigated the effect of increasing the angle of cantilever's inclination and reinforcement ratio on the behavior of rectangular cross-section reinforced concrete beams. The result of the investigation summarized that increasing the angle of cantilever inclination has a little effect on the cracking and ultimate loads, but the overall stiffness of beams which depend on the maximum deflection and maximum strain and highly affected. An increase in the main longitudinal reinforcement ratio led to an increase in the diagonal cracking load, ultimate load, and flexural cracking load, respectively. Kai and Li [6] tested reinforced concrete frames subjected to the loss of the ground corner which represents corner panels. The experimental and analytical study results showed that the loss of the corner column caused the progressive collapse of the frame and plastic hinge developed at the beam end near to the corner joint when using a moderate ratio of transverse reinforcement in the corner joint region .

Rafeeq [7] studied by experimental work the behavior of fixed ends rectangular reinforced concrete beams subjected to the two different types of loading, first one was bending plus shear and the second one was bending and shear plus torsion. The study concluded that the torsional load is substantially reduced the beam load bearing capacity. Thus, if torsional loading is not considered in beam design or the beam has a deficiency

in torsional reinforcement, it is necessary to strengthen the beam. Talaeitaba and Mostofinejad [8] investigated the behavior of fixed supports RC beams under combined shear and torsion. The first case by applying pure shear force, and the other cases was shear plus different value of torsion and the last case was pure torsion. The experimental test results showed that the beam under pure shear has the highest ultimate load of all tested beams and the beam under combined of shear plus high torsion value is the lowest bearing capacity, but the beam under pure torsion has the middle bearing capacity value of them.

Amulu and Ezeagu [9] studied the effect of the combined loadings of torsional moments, bending moments, and shear forces on the behavior of normal strength reinforced concrete beams by using standard design codes and experimental work. This study concluded that the beams failures were due to the combined actions of torsion, shear, and bending moment effects. Therefore, an increase in the capacity of the beams to resist the applied combined loads, were as a result of the increased longitudinal and transverse reinforcements ratio. Also proved that the capacity of the beams can be increased to resist the effects of combined loads by using the amount of reinforcement obtained from torsional design calculations and should be provided in addition to the total amount of bending and shear reinforcement at ultimate loads. Nagendra and Kumar [10] analyzed rectangular reinforced concrete beams with a cantilever L-span under torsional loading by experimental work and numerical analysis to study the effects the reductions of longitudinal and transverse reinforcement on the beams behavior. The beams were provided with reinforcement to resist bending moment and without torsional moment resisting reinforcement. The torsional test is based on the strength of membrane elements subjected to pure shear that was also applied to beams subjected to combined shearing forces, bending moments. The experimental and numerical analysis results showed that the decreasing of longitudinal and transvers reinforcement caused a reducing of beams torsional capacity, but the reducing of longitudinal reinforcement caused the beam failed earlier than beam with reducing of transvers reinforcement.

Most of the researches currently available have been focused on the structural behavior of the beams under the effect of combined loads that loaded by side arms in pure torsion or combined of shear force, bending moment, and torsion moment, but it is too limited or in the otherwise is not available researches about reinforced concrete beam with out of plane parts. As indicated by the best of the authors' knowedge, this study is the first experiment to investigate the structural behavior of beams with the out of plane parts as compared with the straight beam. The main objective of this research is to discover the difference in behavior between the straight beam and the beam containing out of plane parts in its longitudinal path, as well as the effect of the locations and number of these out of plane parts on the structural behavior. Therefore, a laboratory result was obtained proved that the classical method of design of straight beam needs to be modified including the torsional effect resulting from existing out of plane parts, and their failure mode was different and their load bearing capacity was also less than the straight beam.

## 2. EXPERIMENTAL PROGRAM

**2. 1. Specimens Preparation** In this paper, all reinforced normal strength concrete beams with one, two, and three out of plane parts and straight control beam were fabricated and loaded with a constant a/d ratio of 2.647. All tested specimens had a total span 2000 mm and effective span 1500 mm with rectangular cross-section of 150 mm width, 200 mm depth. The beams description and their material hardened properties are summarized in Table 1. All specimens were designed according to ACI Code [11], the reinforcement cage include six deformed longitudinal bars of a 12mm diameter, and 8mm diameter bars as square ties with $135^0$ minimum inside bend standard hook with a uniformly spaced 81mm center to center along the beams length, as shown in Figure 2. The

**TABLE 1.** The beams label and their material hardened properties

| Symbols | Refer to | Splitting tensile strength (MPa) | Flexural Tensile Strength (Modulus of Rupture) (MPa) | Average concrete compressive strength at 28 days (MPa) |
|---|---|---|---|---|
| NSC-S | Normal Strength Concrete Straight Beam | 2.56 | 7.37 | 35 |
| NSC-1OP | Normal Strength Concrete Beam with One Out of Plane Part | 2.56 | 7.37 | 35 |
| NSC-2OP | Normal Strength Concrete Beam with Two Out of Plane Part | 2.56 | 7.37 | 35 |
| NSC-3OP | Normal Strength Concrete Beam with Three Out of Plane Parts | 2.56 | 7.37 | 35 |

*Standard cylinders (150mm×300 mm) were used to evaluate the compressive strength of concrete.

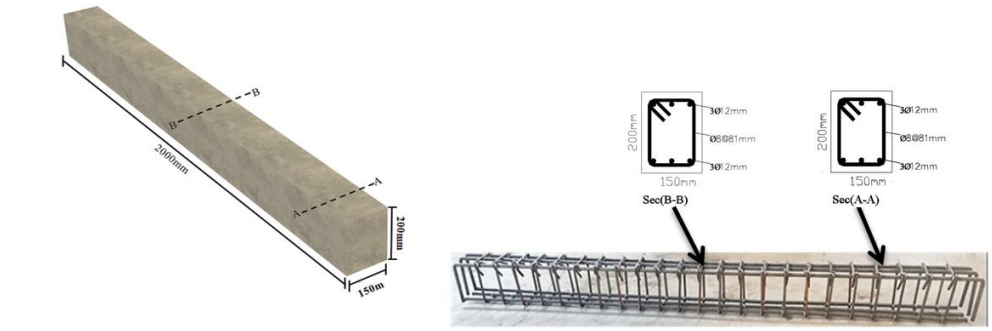


(a) Geometry and reinforcement of NSC-S beam

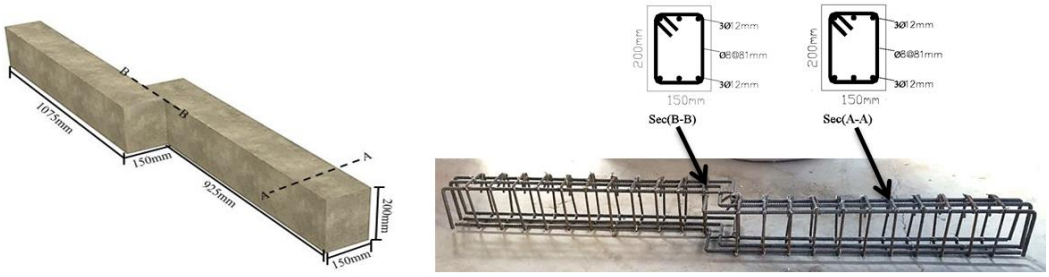


(b) Geometry and reinforcement of NSC-1OP beam

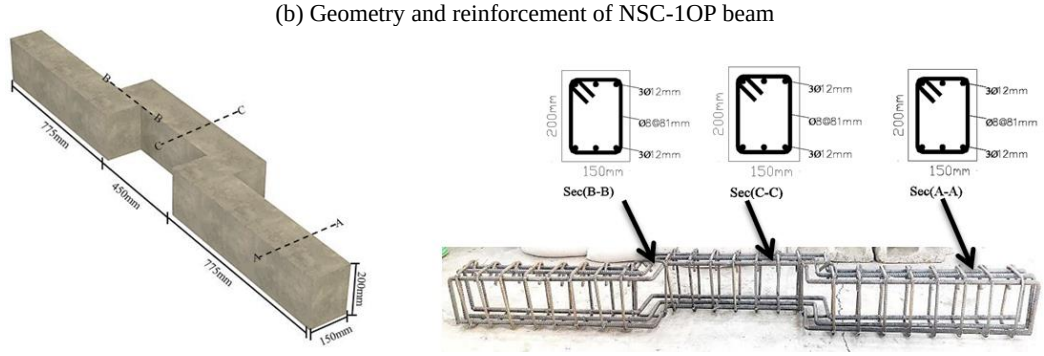


(c) Geometry and reinforcement of NSC-2OP beam

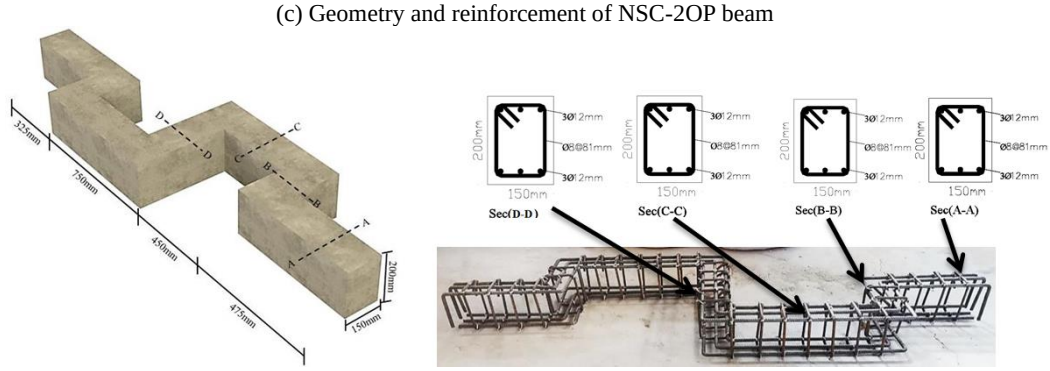


(d) Geometry and reinforcement of NSC-3OP beam

**Figure 3.** Geometry and reinforcement details of tested beams

reinforcement cage was incorporated into plywood molds and using 160 mm concrete spacers as a concrete cover from all sides. The tensile yield strengths for 8 mm and 12 mm bars were 559 and 413 MPa, respectively. The flexural tensile strength was estimated for the prisms of dimensions (100×100×400) mm according to ASTM C78-02 [12]. The tensile strength also measured by splitting tensile strength for concrete cylinders of (100 mm diameter ×200 mm length) according to ASTM C496/C 496M-04 [13].

The longitudinal and transverse reinforcement that used in the beams with out of plane part was the same that used in the control straight beam. The control beam designed according to ACI Code [11] based on its own of bending moment and shear force. The longitudinal reinforcement of flexural behavior was used as a

constant ratio of 0.011 for a negative and positive moment and then the required transverse tie reinforcement was calculated and the ultimate load that was expected to applied in the experimental work. The analytical equations based on the case that shown in Figure 3 and used to calculate the required applied load and the required transverse reinforcement as below:

$$R_A = V_A = R_B = V_B = P \quad (1)$$

$$M_A = M_B = \frac{P.a(L-a)}{L} \quad (2)$$

$$M_C = M_D = \frac{P.a^2}{L} \quad (3)$$

where; P is the applied load, $R_A$ and $R_B$ is the reactin at suupports, $V_A$ and $V_B$ is the shear force at suupports, and L is the effctive span of beam.

Then substitute these equations into the ACI Code [11] design equations to calculate the applicable ultimate load (P) at supports and mid span as below:

(a) Calculate nominal strength bending moment as:

$$M_n = A_s.f_y\ (d - \frac{a}{2}) \quad (4)$$

(b) Calculations of ultimate load at supports by equating the nominal bending moment strength to the applied load bending moment at point A or B as:

$$M_n = M_A + M_{D.L} = \frac{P.a(L-a)}{L} + \frac{W_{Self}.L^2}{12}$$
$$P_{Max} = \frac{M_n.L}{a(L-a)} - \frac{W_{Self}.L^3}{12a(L-a)} \quad (5)$$

(c) Calculations of ultimate load at mid span by equating the nominal strength bending moment to the applied load bending moment at point C or D as:

$$M_n = M_C + M_{D.L} = \frac{P.a^2}{L} + \frac{W_{Self}.L^2}{24}$$
$$P_{Max} = \frac{M_n.L}{a^2} - \frac{W_{Self}.L^3}{24\,a^2} \quad (6)$$

where; $M_n$ is the nominal bending moment, $M_C$ is the live load bending moment at loading point, $M_{D.L}$ is the dead load bending moment, $W_{self}$ is the beam self-weight, $A_s$ is the area of reinforcement, $f_y$ is the yield strength of reinforcement, d is the effective depth of beam, ɑ is the shear span, and a= compression stress block depth = $\frac{A_s f_y}{0.85 f c' b}$.

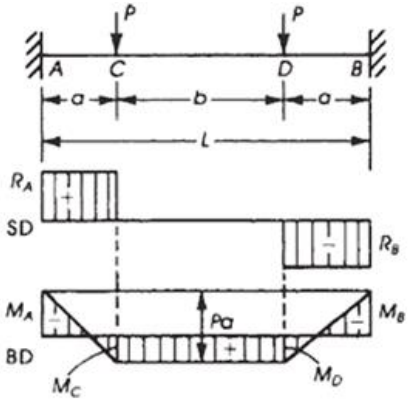


**Figure 3.** Fixed ends beam aid

The shear reinforcement required and their spacing was calculated as follows:

$$ØV_C = 0.75 b_w d \frac{\sqrt{f_c'}}{6} \quad (7)$$

$$V_S = \frac{1}{Ø}(V_U - ØV_C) \quad (8)$$

$$S = \frac{A_v f_y d}{V_S} \quad (9)$$

Check for maximum spacing to provide Av as:

$$S = \begin{cases} \frac{16\,A_v f_y}{b_w d\sqrt{f_c'}} \\ \frac{3A_v f_y}{b_w} \\ \frac{d}{2} \\ 600 \end{cases} \quad (10)$$

where; $V_C$ is the Shear strength of concrete, $V_U$ is the shear force due to applied loads, $b_w$ is beam width, $A_v$ is the total area of shear reinforcement within a spacing S, $V_S$ is the shear reinforcement strength, S is the spacing between stirrups or ties.

All the beams without of plane parts reinforced with the same reinforcement of the control straight beam in flexural and shear.

The beams in this study were fabricated by using normal strength concrete (NSC) that designed according to ACI Committee 211.1-01[14] by using an ordinary Portland cement, natural clean sand, partial crashed coarse aggregate with maximum size 12mm, and water, as shown in Table 2.

The properties of fresh concrete were found by workability slump flow test and fresh density and shown in Table 3; while the hardened properties evaluated by compressive strength, splitting tensile strength, and flexural tensile strength test as mentioned in Table 1.

**TABLE 2.** Mix design to produce 1m$^3$ of normal strength concrete.

| Cement (kg) | Fine aggregate (kg) | Coarse aggregate (kg) | Water (kg) |
|---|---|---|---|
| 400 | 818.16 | 946 | 214.6 |

**TABLE 3.** The properties of fresh concrete test results

| Concrete Type | Slump flow (mm) | Fresh density (Kg/m$^3$) |
|---|---|---|
| NSC | 60 | 2422 |

The models were prepared to compare the structural behavior of NSC beams with out of plane part with a control NSC-S beam to evaluate the effect of the number and location of these out of plane parts on their structural behavior as compared with the straight beam.

**2. 2. Test Setup and Instrumentation** The tested beams were supported by using a special clamping steel frame of HP section which clamped to ends of the beams as shown in the schematic drawn in Figure 4 and experimental test set up in Figure 5. A

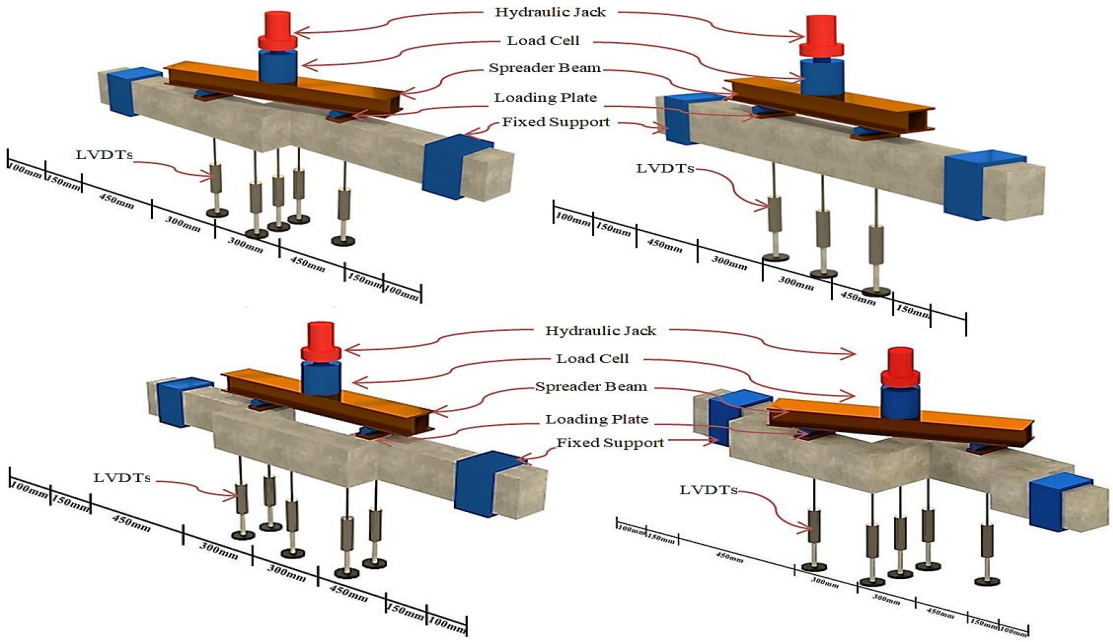


**Figure 4.** Schematic of Test set up

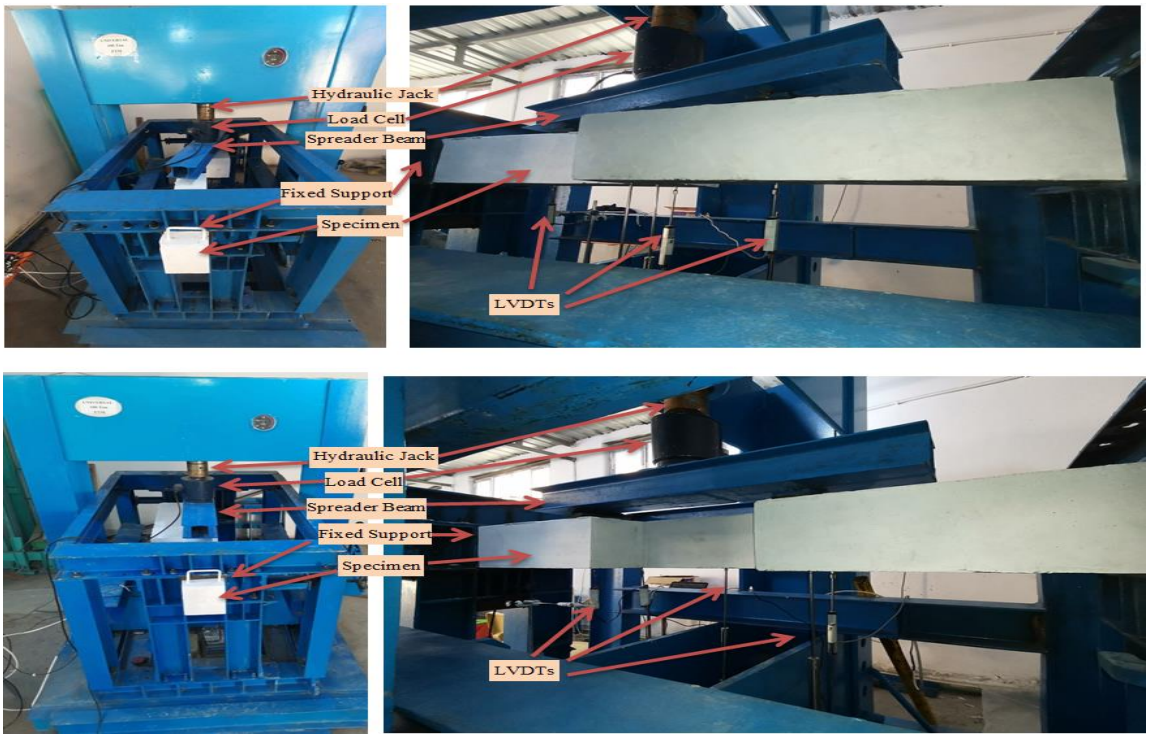


**Figure 5.** Experimental Test set up

clear span of 1500 mm between the supports was loaded with a two-point load to evaluate the structural performance of the beams. The shear span to effective depth (a/d) ratio was fixed value by using a distance of 450mm from the loading point to the interior face of support. The length of the flexural span between the loading points is equal to 600 mm. The universal test machine with a hydraulic jack of 1000 KN capacity were used to applied the load with gradually increments of 5 KN up to failure. The load was monitored by installing the load cell between the jack and a spreader stiff beam. The deflection at mid span and under the loading points was monitored by using electrical LVDTs were positioned vertically under the beams. The angle of twist at the mid span of beams was measured by taking the difference between readings of back and front LVDTs and divided by the distance between them and using trigonometric functions.

All the test devices described above were connected to an electrical data logger that was computerized to readings and saving the data per second n the course of experimental run.

## 3. EXPERIMENTAL RESULTS

### 3. 1. General Behavior and Crack Patterns

The development of cracks at each stage of loading was measured and marked on the beams to observe the growth, sequence, and pattern of cracking during the test up to the specimen's failure. The beams' cracks patterns at the failure load after rleas load are shown in Figure 6 and their failures before release the load are shown in Figure 7. The specimens with one and two out of plane part were failed in the torsion at out of plane part then followed by flexure mode at the fixed supports. The specimen with three out of plane parts was failed in the torsion at out of plane parts. In general, the torsional cracks of beams were started at the interior corners of out of plane parts and continued from bottom to the top then distributed at the top face of beam in the mid span region and at the side faces of the out of plane parts, while the flexural and other torsional cracks observed bellow the point load and at the shear span (a), and flexural cracks at the supports.

The torsional and flexural cracks increased, widened, and traveled with increasing the applied load. In NSC-1OP the torsional cracks started at the out of plane part then followed by vertical flexural and inclined torsional cracks below the point load and inclined torsional cracks at the shear span (a), then finally flexural cracks at the support. In NSC-2OP the first cracks appear at the interior corner of out of plane parts then flowed be vertical flexural cracks at mid span and at last, the negative moment cracks started at the supports. NSC-3OP torsional cracks were started at the out of plane parts and below the point load, and then followed by the combined torsional and flexural cracks at the supports. The cracks propagated from the corners to the faces of out of plane parts in diagonal shape and increase in their width at the same time increasing number of support cracks up to the beam failure. In NSC-S the first vertical flexural cracks appeared at the mid span and at the fixed supports then followed by the vertical flexural cracks under the loading points and at last, the inclined shear cracks appeared at the shear span (a).


**Figure 6.** Experimental crack patterns of specimens at the failure load


**Figure 7.** Specimens behavior at the failure load

Finally, at the failure load, the flexural cracks at the fixed support rapidly expanded and almost reached to the bottom face of the beam, followed by the concrete crushing at the mid span region. It is worth mentioning that the cracking load of NSC-S was highest among them and NSC-3OP was lowest, but NSC-1OP and NSC-2OP were of approximation the same value. The cracking and ultimate loads for beams are plotted in Figure 8 and the maximum cracks width at the ultimate load are plotted in Figure 9. The cracks under different loading characteristics are shown in Figure 10.

### 3. 2. Load-deflection Characteristics

**3. 2. 1. General Behavior** The load-deflection response of all the tested beams for measured deflection at mid span is shown in Figure 11. This response is the main result to evaluate each of the ductility, energy absorption, and stiffness. From the curves it can be revealed that the NSC-S beam has the highest ultimate load of all the beams without of plane parts and less central deflection. It is worth to mention that the NSC-2OP beam has ultimate load higher than the NSC-1OP and NSC-3OP beams. This behavior due to the axis of the mid span part of NSC-2OP beam is parallel to the beam axis and decreased the applied torsional moment at this part which led to increase the load-carrying capacity, while the NSC-1OP and NSC-3OP have mid span part perpendicular to the beam axis and increase torsional moment at these parts which led to decrease the load-carrying capacity.

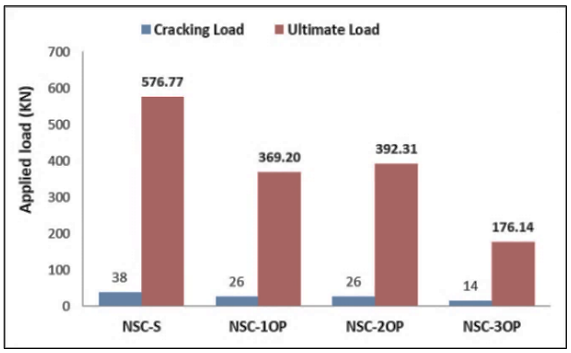


**Figure 8.** Cracking and ultimate loads of beams

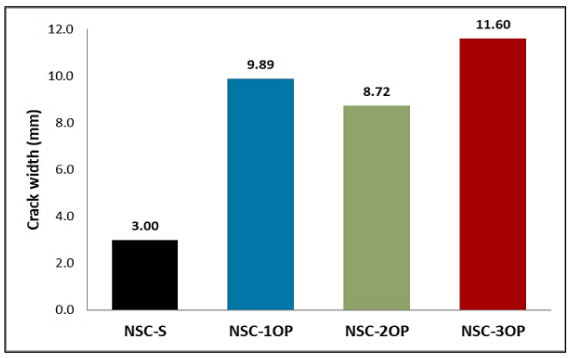


**Figure 9.** Maximum cracks width at the ultimate load

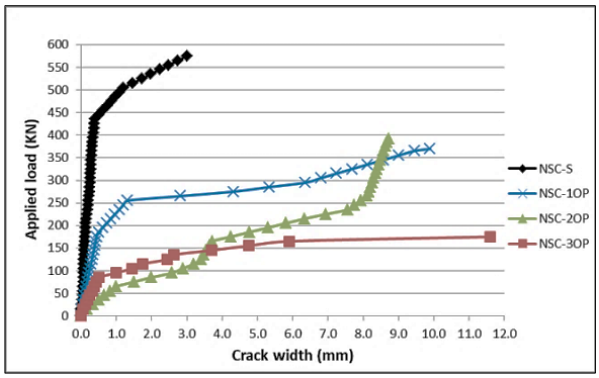


**Figure 10.** Load and crack with response of specimens

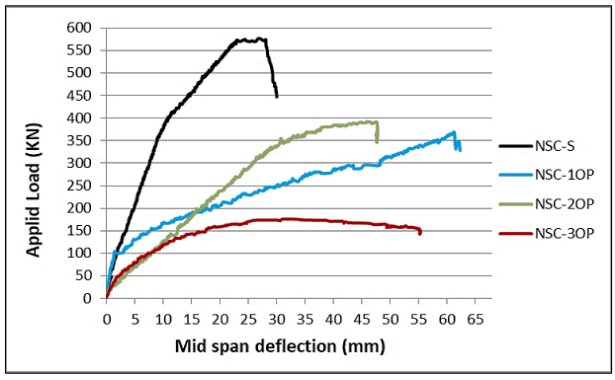


**Figure 11.** Load and mid span deflection response of specimens

The relations between the loads and deflections also can be described by the beam deflection shapes along the span between the supports as shown in Figure 12. The deflection shape at the ultimate load was carried out in the experimental work by taking the readings of LVDTs that installed under the mid span point and under the loading points.

From the load-mid span deflection and deflection shape responses it can be summarized that the NSC-S beam has an ultimate load 35.96%, 33.33%, and 69.46% higher than NSC-1OP, NSC-2OP, and NSC-3OP beam, respectively. The mid span deflection of NSC-1OP, NSC-2OP, and NSC-3OP beam was higher than NSC-S beam by 56.23%, 47.68%, and 45.99%, respectively. These results gave indicate that the increase number of out of plane parts reduced the deflection at the ultimate load and made the deflection shape is close to the shape of the NSC-S beam. The ultimate load capacities, related deflection, and failure mode of all the tested beams are summarized in Table 4.

### 3. 2. 2. Displacement Ductility Index

Among many aspects required in reinforced concrete structural members design, ductility has become involuntary by the standard codes ACI 318, EUROCODE 8, and ABNT NBR 6118 [15-17]. In this context, Shadmand et al. [18] mentioned that the ductility represents the one of the materials properties which can be defined as the ability of material or a

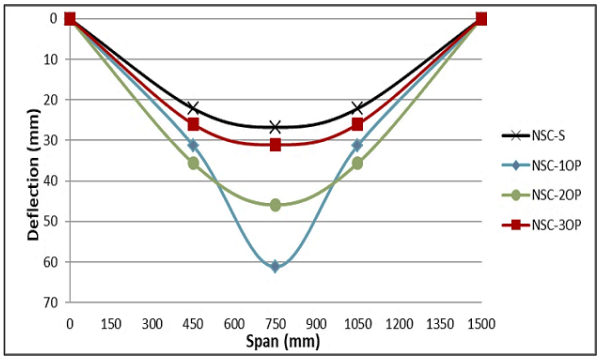


**Figure 12.** Deflection shape response of specimens

**TABLE 4.** The experimental results output of all the tested beams

| Beams | Failure load $P_U$ [kN] | Mid span deflection $\Delta_U$ (mm) | Yield load $P_y$ [kN] | Mid span deflection $\Delta_y$ (mm) | Ductility index | Energy absorption (KN.mm) | Energy ductility index | Failure mode |
|---|---|---|---|---|---|---|---|---|
| NSC-S | 576.76 | 26.79 | 432.57 | 13.45 | 2.05 | 11924.52 | 2.19 | Flexure at support and mid span |
| NSC-1OP | 369.36 | 61.21 | 277.02 | 36.00 | 1.71 | 15283.11 | 1.14 | Torsion at out of plane part |
| NSC-2OP | 392.30 | 45.92 | 294.22 | 25.39 | 1.81 | 12147.94 | 1.90 | Torsion at out of plane part and flexure at support |
| NSC-3OP | 176.14 | 31.09 | 132.10 | 11.57 | 2.69 | 7929.77 | 3.43 | Torsion at all the out of plane parts |

member to undergo large deformations without significant resistance loss or rupture before collapse. In concrete structural members, it is can be obtained by the ratio of steel reinforcement within it; because mild steel is a ductile material that can be bent and twisted without rupture [19,20]. Ductility of structural member in experimental work can be estimated in terms of ductility index.

According to Kim et al, [21], Maghsoudi and Bengar [22] and Faez et al. [23] ductility index is defined as follows:

$$\mu = \frac{\Delta_U}{\Delta_y} \quad (11)$$

where; μ is the ductility index, $\Delta_U$ is the defection of the beam at the ultimate load, and $\Delta_y$ is the defection of the beam at the yield load.

Researchers proposed several approaches to evaluate this term; while Park [24-25] depended on the equivalent elasto-plastic yield point that depends on the equivalent elasto-plastic energy absorption;, otherwise used the ultimate load deflection at the first fracture of any element that occurs at the end of the elastic zone and causes reduction in stiffness as shown in Figure 13. In this strategy, the yield point deflection (Δy) is represent the intersection point of two lines; the first line is a horizontal tangent to the load-deflection curve at the ultimate load, whilst the second one is a line passing through the origin point to the point that represents 75% of the ultimate load.

The deflections at the yield and ultimate loads as well as the ductility indexes of all beams are listed in Table 4 and plotted in Figure 14. As can be seen from this table and figure that the ductility of NSC-1OP and NSC-2OP was less than NSC-S by 16.58% and 11.70%, respectively, while NSC-3OP is 23.79% higher than NSC-S. Furthermore, it can be seen that increasing number of out of plane parts improved the ductility and reduced the difference with NSC-S. Moreover, these indications explained by relative ductility indexes that evaluated for the beams with out of plane parts relative to the control straight beam as plotted in Figure 15.

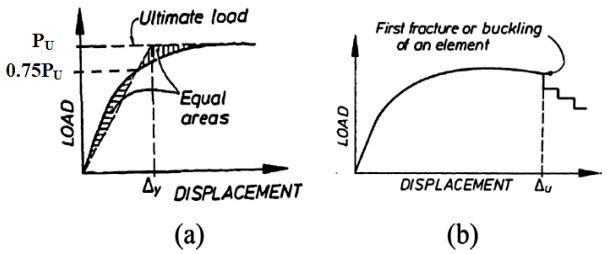


**Figure 13.** Park definition for displacements [19, 20]: (a) yield displacement by equivalent elasto-plastic energy absorption. (b) The ultimate deflection is based on the first fracture of an element

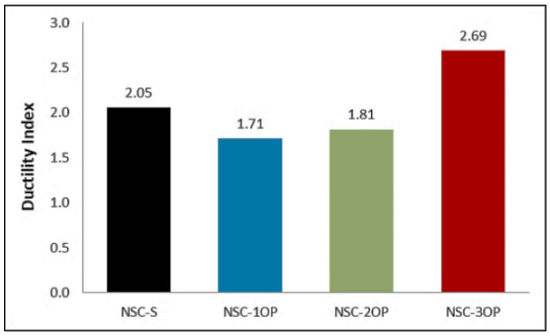


**Figure 14.** Beams ductility index

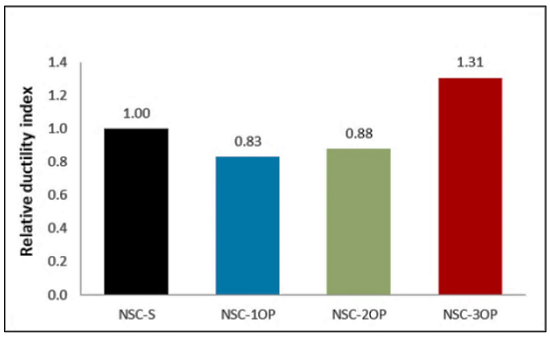


**Figure 15.** Beams relative ductility index

**3. 2. 2. Energy Ductility Index** The energy absorption capacity of the concrete beam can be approximated as the area under the load-deflection curve up to its ultimate load, which represents the energy absorption that could sustain before displaying a significant drop in load carrying capacity [26-28]. Absorbed energy can be obtained by integrating the area at each loading step in load-displacement relationship [29-32]. Figure 16 represent the load-deflection curve where; the total energy *E* done by integrate the product the magnitude of the load *P* and of the small deflection *dx* and which is equal to the area under the load-deformation diagram between x = 0 and x = $x_1$ and can be written as:

$$E = \int_0^{x_1} P\, dx \quad (12)$$

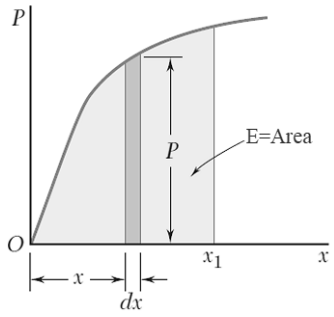


**Figure 16.** Determination of energy based ductility capacity

The calculations of the area under the load-deflection curves for all tested beams are illustrated in Figure 17 and summarized in Table 4. The results showed that the NSC-1OP beam has the highest value of energy absorption and this value decreased when the number of out of plane parts increased as compared with the straight beam.

Thomsen et al. [32], Maghsoudi and Bengr [33] defined the energy ductiliy index as ($\mu_E$) which is the ratio between the energy of the system at failure ($E_u$) and the energy of the system at yielding load of tensile steel reinforcement at the central support ($E_y$):

$$\mu_E = \frac{E_u}{E_y} \quad (13)$$

where $E_u$ is the failure energy of the beam at ultimate load, $E_y$ is the elastic energy at first steel yield load as shown in Figure 18, and $\mu_E$ is the energy ductility index.

The energy ductility index that estimated according to Equation (13) for the tested beams are plotted in Figure 19.

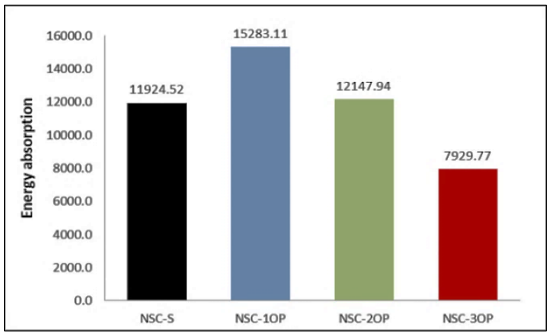


**Figure 17.** Beams total energy absorption

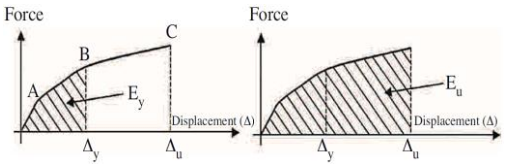


**Figure 18.** Determination of energy based ductility capacity

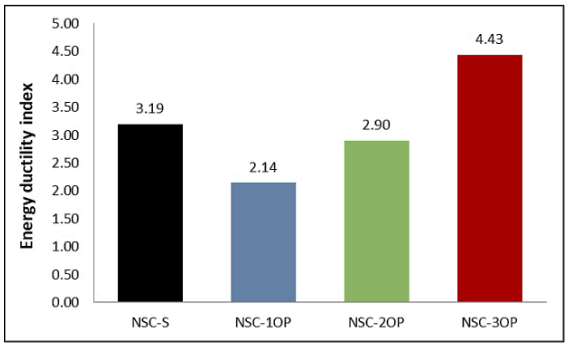


**Figure 19.** Beams energy ductility indexes

Abdulraheem [34] proposed approach to evaluate the ability of RC beams to absorb the energy in terms of energy ductility index $\mu_{en}$ by classified the total energy absorption into two regions, elastic energy zone $E_{el}$ and plastic energy zone $E_{PL}$ and can be estimated as the ratio of the plastic energy to the elastic energy as shown in Figure 20, and calculated using the following equation:

$$\mu_{en} = \frac{E_{Pl}}{E_{el}} = \frac{E_{total} - E_{el}}{E_{el}} \quad (14)$$

where $E_{pl}$ is the plastic energy that represents the area under the load-deflection curve from the yielding point up to the ultimate load, and $E_{el}$ is the elastic energy that represents the area under the linear part of the load-deflection curve up to the yielding point as shown in Figure 20.

In this study, Equation (14) used to estimate the energy absorption index for the tested beams, becase it gave results more acceptable as copare with the displacemnt ductility index. The estimated results are summarized in Table 4 and plotted in Figure 21.

**3. 2. 3. Twisting Angle** The angle of twist for the cross-sections at the mid span was calculated at each stage of load increase in the experiment up to the beam rupture. The angle was measured by taking the maximum absolute different readings between the LVDTs that installed at the at front and back points and the LVDT at centerline of the beam which installed as

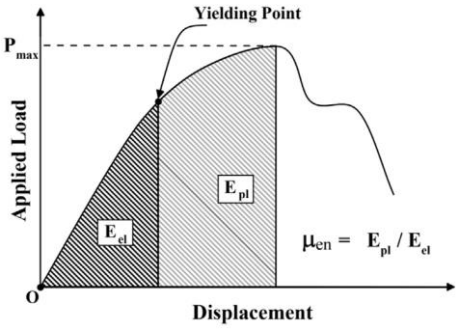


**Figure 20.** Procedure of energy absorption index Evaluation

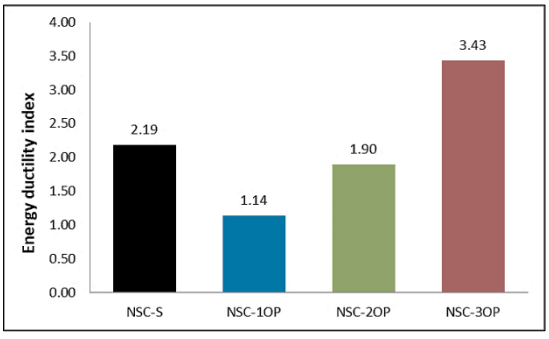


**Figure 21.** Beams energy ductility indexes

shown in Figure 4, then divided on the distance between them and took the average of front and back angles. The load and mid span twisting response is explained in Figure 22.

The load-mid span rotation response used to study the effect of increase number of out of plane parts and their locations on the beams rotational behavior. It can be observed that the NSC-2OP beam has the angle of twist at the ultimate load higher than NSC-1OP and NSC-3OP beams by 27.32% and 38.59%. That means the perpendicular direction of mid span part to the beam axis has a greatly effect on the decreasing of the angle of twist, especially when increase the number of out of plane parts. The beams twisting angle at service and ultimate load are addressed in Table 5 and plotted in Figure 23.

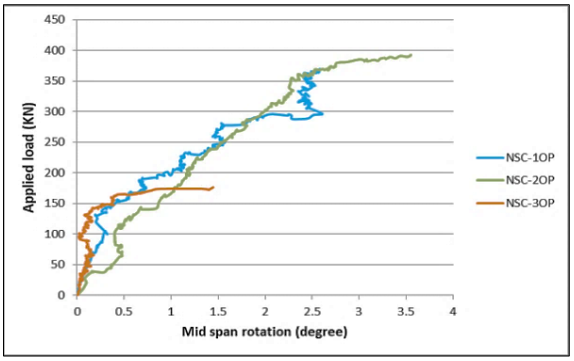


**Figure 22.** Applied load versus twisting angle of the beams

**TABLE 5.** The mid-span twisting angle of all the tested beams

| Beams | * Twisting angle at service load (degree) | Twisting angle at ultimate load (degree) |
|---|---|---|
| NSC-1OP | $1.56^0$ | $2.58^0$ |
| NSC-2OP | $1.80^0$ | $3.55^0$ |
| NSC-3OP | $1.10^0$ | $2.18^0$ |

*Service load = 65% ultimate load

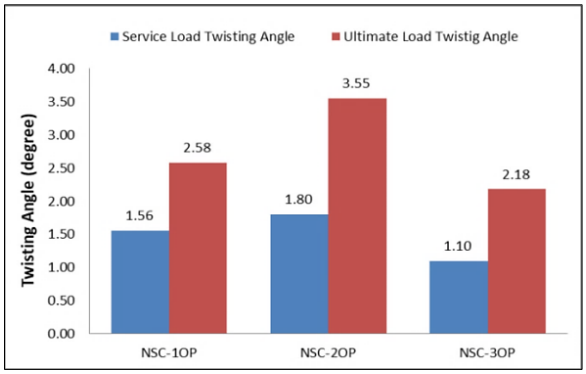


**Figure 23.** Twisting angle of beams at service and ultimate load

## 4. CONCLUSIONS

Based on the experimental investigations, the effect of the out plane part on the structural behavior of straight and with out of plane part RC beams subjected to static loads are examined. The following are the most important notices for observed and recorded results:

1. The presence of out of plane part decreased the load-bearing capacity of all the beams with out of plane part beam as compared with the straight beam by 35.96%, 33.33%, and 69.46%.
2. The ductility of the beams that estimated by displacement ductility index and energy ductility index methods gave indication that the ductility of the beams with out of plane parts increased when increasing the number of these out of plane parts until to reach and pass the ductility of the straight beam when using beam with three out of plane parts.
3. The cracks width- load characteristics were affected by the number and loaction of out of plane parts and the maximum crack width of the straight beam is the smallest one and the crack of the beams was affected by the location and direction of the out of plane part relative to the axis of beam at mid span, because the maximum crack width of the beam with two out of plane parts is smaller than of the beams with one and three out of plane parts.
4. The angle of twist of the beams was also affected by the location and direction of the out of plane part relative to the axis of the beam at mid span, because the twisting angle of the beam with two out of plane parts is higher than of the beams with one and three out of plane parts at the service and ultimate load.
5. The failure mode of beams with one and two out of plane parts was occurred by torsional cracking propagation at the out of plane part and torsional and flexural cracks at the other spans and at the supports faces, and the beam with one and three out of plane parts was failed by torsional cracks propagation at the out of plane parts, while the straight beam was failed by flexural cracks at the mid span and at the supports.

From the study conclusions above, it can be seen that the load bearing capacity and the structural behavior of beams with out of plane parts was affected by the number and locations of the out of plane parts.

## 5. REFERENCES

1. Owainati, S. A. R. "Behaviour of reinforced concrete beams under torsion, bending and shear." (1973). https://spiral.imperial.ac.uk/handle/10044/1/20540
2. Ali, Mohamad, and A. Anis. "Strength and behaviour of reinforced concrete spandrel beams." KB thesis scanning project 2015 (1983). http://hdl.handle.net/1842/12664

3. Kamiński, M., and W. Pawlak. "Load capacity and stiffness of angular cross section reinforced concrete beams under torsion." ***Archives of civil and Mechanical Engineering***, Vol. 11, No. 4 (2011): 885-903. doi: 10.1016/S1644-9665(12)60085-5.
4. ACI-ASCE Committee 445. ***" Report on Torsion in Structural Concrete"*** American Concrete Institute of the Advancing concrete knowledge, No IR12 (2013). https://www.amazon.com/ACI-445-1R-12-Torsion-Structural-Concrete-ebook/dp/B00E4VDIV4
5. Elsayed. A. A., Noaman. M., Abdallah. M. A. M., Abdelrahim. M. A. A. "Behavior of R.C. Beams with Inclined Cantilever." IOSR Journal of Mechanical and Civil Engineering, Vol. 12, No. 4, (2015), 74-96. doi: 10.9790/1684-12427496
6. Qian, Kai, and Bing Li. "Performance of three-dimensional reinforced concrete beam-column substructures under loss of a corner column scenario." ***Journal of Structural Engineering,*** Vol. 139, No. 4, (2013), 584-594. doi:10.1061/(asce)st.1943-541x.0000630.
7. Rafeeq, Ranj. "Torsional Strengthening of Reinforced Concrete Beams Using CFRP Composites." (2016). doi:10.15760/etd.3121.
8. Talaeitaba, Sayed Behzad, and Davood Mostofinejad. "Fixed supports in assessment of RC beams' behavior under combined shear and torsion." ***International Journal of Applied***, Vol. 1, No. 5, (2011), http://www.ijastnet.com/journals/Vol_1_No_5_September_2011/15.pdf
9. Amulu, C. P., and C. A. Ezeagu. "Experimental and analytical comparison of torsion, bending moment and shear forces in reinforced concrete beams using BS 8110, euro code 2 and ACI 318 provisions." ***Nigerian Journal of Technology***, Vol. 36, No. 3, (2017), 705-711. doi: 10.4314/njt.v36i3.7.
10. Nagendra Prasad. N and Naresh Kumar. Y, "Torsional behavior of reinforced concrete 'L' beam, International journal of advanced research in basic engineering science and technology, ISSN: 2456-5717, Vol. 3, Special issue 35, (2017).
11. American Concrete Institute (ACI), ACI 318-319: building code requirements for structural concrete, Farmington Hills, (2019). doi: 10.2307/3466335.
12. Standard, A. S. T. M. "C78. 2002. Standard test method for flexural strength of concrete (using simple beam with third point loading)." Annual Book of ASTM Standards, Vol. 4, No. 2, (2002). doi: 10.1520/c0078-02
13. Astm, C. "496/C 496M-04." Standard test method for splitting tensile strength of cylindrical concrete specimens, Vol. 4 (2004), 5. doi: 10.1520/c0496_c0496m-04
14. Dixon, Donald E., Jack R. Prestrera, George RU Burg, Subcommittee A. Chairman, Edward A. Abdun-Nur, Stanley G. Barton, Leonard W. Bell et al. "Standard Practice for Selecting Proportions for Normal, Heavyweight, and Mass Concrete (ACI 211.1-91)." (1991), 1-38. https://kashanu.ac.ir/Files/aci%20211_1_91.pdf.
15. Brazilian Association of Technical Standards NBR 6118 2014 - Design of Concrete Structures - Procedure. Rio de Janeiro, ABNT. 2014. doi: 10.1590/s1983-41952015000400008
16. ACI Committee. "Building code requirements for structural concrete:(ACI 318-02) and commentary (ACI 318R-02)." American Concrete Institute, 2002. https://hoseinzadeh.net/ACI-318-02.pdf
17. Code, Price. "Eurocode 8: Design of structures for earthquake resistance-part 1: general rules, seismic actions and rules for buildings." Brussels: European Committee for Standardization (2005). https://www.phd.eng.br/wp-content/uploads/2015/02/en.1998.1.2004.pdf
18. Shadmand, M., A. Hedayatnasab, and O. Kohnehpooshi. "Retrofitting of Reinforced Concrete Beams with Steel Fiber Reinforced Composite Jackets." ***International Journal of Engineering, Transactions B: Applications,*** Vol. 33, No. 5 (2020), 770-783. doi: 10.5829/ije.2020.33.05b.08.
19. Punmia, B. C. *Reinforced Concrete Structures* Vol. I. Vol. 1. Firewall Media, 1992. https://books.google.ps/books?id=6g1fu4pRDCkC
20. Khamees, Shahad S., Mohammed M. Kadhum, and Nameer A. Alwash. "Effect of hollow ratio and cross-section shape on the behavior of hollow SIFCON columns." ***Journal of King Saud University-Engineering Sciences***, Vol. 33, No. 3 (2021): 166-175. doi: 10.1016/j.jksues.2020.04.001 .
21. Kim, Sung Bae, Na Hyun Yi, Hyun Young Kim, Jang-Ho Jay Kim, and Young-Chul Song. "Material and structural performance evaluation of recycled PET fiber reinforced concrete." ***Cement and Concrete Composites***, Vol. 32, No. 3, (2010), 232-240. doi:10.1016/j.cemconcomp.2009.11.002 .
22. Maghsoudi, A. A., and H. Akbarzadeh Bengar. "Acceptable lower bound of the ductility index and serviceability state of RC continuous beams strengthened with CFRP sheets." ***Scientia Iranica***, Vol. 18, No. 1, (2011), 36-44. doi: 10.1016/j.scient.2011.03.005 .
23. Faez, A., A. Sayari, and S. Manei. "Retrofitting of RC Beams using Reinforced Self-compacting Concrete Jackets Containing Aluminum Oxide Nanoparticles." ***International Journal of Engineering, Transactions B: Applications,*** Vol. 34, No. 5, (2021), 1195-1212. **doi**: 10.5829/ije.2021.34.05b.13.
24. Park, R. "Ductility evaluation from laboratory and analytical testing." In Proceedings of the 9th world conference on earthquake engineering, Tokyo-Kyoto, Japan, Vol. 8, 605-616.1988. https://www.iitk.ac.in/nicee/wcee/article/9_vol8_605.pdf.
25. Park, Robert. "Evaluation of ductility of structures and structural assemblages from laboratory testing." ***Bulletin of the New Zealand Society for Earthquake Engineering***, Vol. 22, No. 3, (1989), 155-166. doi: 10.5459/bnzsee.22.3.155-166.
26. Jaafer, Abdulkhaliq Abdulyimah. "Experimental investigation on the ferrocement slabs with a sifcon matrix." Wasit Journal of Engineering Sciences 3, No. 1, (2015), 40-54. doi: 10.31185/ejuow.vol3.iss1.34.
27. Goldston, Matthew, A. Remennikov, and M. Neaz Sheikh. "Experimental investigation of the behaviour of concrete beams reinforced with GFRP bars under static and impact loading." ***Engineering Structures***, Vol. 113, (2016), 220-232. doi: 10.1016/j.engstruct.2016.01.044.
28. Jomaah, Muyasser M., and Diyaree J. Ghaidan. "Energy Absorption Capacity of Layered Lightweight Reinforced Concrete Beams with Openings In Web." ***Civil Engineering Journal***, Vol. 5, No. 3, (2019), 690-701. doi: 10.28991/cej-2019-03091279
29. Ohno, Tomonori, and Takashi Nishioka. "An experimental study on energy absorption capacity of columns in reinforced concrete structures." ***Doboku Gakkai Ronbunshu***, No. 350, (1984), 23-33. doi: 10.2208/jscej.1984.350_23.
30. Beer, Ferdinand P., Elwood Russell Johnston, John T. DeWolf, and David F. Mazurek. ***Mecânica dos materiais***. Amgh, 2011.
31. Yu, R., P. Spiesz, and H. J. H. Brouwers. "Energy absorption capacity of a sustainable Ultra-High Performance Fibre Reinforced Concrete (UHPFRC) in quasi-static mode and under high velocity projectile impact." ***Cement and Concrete Composites***, Vol. 68, (2016), 109-122. doi: 10.1016/j.cemconcomp.2016.02.012
32. Thomsen, Henrik, Enrico Spacone, Suchart Limkatanyu, and Guido Camata. "Failure mode analyses of reinforced concrete beams strengthened in flexure with externally bonded fiber-

reinforced polymers.", ***Journal of Composites for Construction,*** Vol. 8, No. 2, (2004), 123-131. doi: 10.1061/(asce)1090-0268(2004)8:2(123).

33. Maghsoudi, A. A., and H. Akbarzadeh Bengar. "Moment redistribution and ductility of RHSC continuous beams strengthened with CFRP." ***Turkish Journal of Engineering and Environmental Sciences***, Vol. 33, No. 1, (2009), 45-59. doi: 10.3906/muh-0901-6.

34. Abdulraheem, Mustafa S. "Experimental investigation of fire effects on ductility and stiffness of reinforced reactive powder concrete columns under axial compression." ***Journal of Building Engineering,*** Vol. 20, (2018), 750-761. doi: 10.1016/j.jobe.2018.07.028

## Persian Abstract

**چکیده**

هدف از این مقاله بررسی و مقایسه رفتار ساختاری تیر مستقیم بتن آرمه و سایر تیرهای ساخته شده در آنجا با یک ، دو و سه قسمت خارج صفحه است. این مطالعه بر روی تأثیر تعداد و محل قطعات صفحه خارج بر روی انحراف و بازتاب دهانه میانه تیرها ، و همچنین شاخص شکل پذیری ، بارهای ترک خوردگی و حالت های خرابی متمرکز شده است. چهار تیر با عرض مقطع ۱۵۰ میلی متر و عمق ۲۰۰ میلی متر و طول ۲ متر ساخته شده است. تمام تیرها با بتن با مقاومت نرمال و نسبت تقویت طولی ثابت ۰.۰۱۱ برای گشتاورهای منفی و مثبت ساخته شده اند. تمام نمونه های پرتو توسط انتهای ثابت فولادی گیر شده و تحت شکست دو نقطه ای قرار گرفتند. نتایج به دست آمده نشان داد که ظرفیت تحمل بار تیر مستقیم بیشتر از تیرهای خارج از قطعات صفحه است. بعلاوه ، پرتوی دارای دو قسمت از صفحه دارای ظرفیت بالاتر از پرتوهای دارای یک و سه قسمت از صفحه به ترتیب ۵.۸۶ و ۵۵.۰۷٪ است. علاوه بر این ، نتایج نشان داد که انعطاف پذیری با افزایش تعداد قطعات خارج صفحه ۵.۵۲٪ و ۳۲.۷۱٪ در مقایسه با پرتو با قسمت خارج صفحه افزایش می یابد.